ARTICLE NO. 79-0142R

J80-013

20005
20017

Numerical Study of Strong Slot Injection into a Supersonic Laminar Boundary Layer

Michele Napolitano*
University of Cincinnati, Cincinnati, Ohio

This paper addresses the problem of strong slot injection into a supersonic laminar boundary layer within the framework of triple-deck theory. A previous numerical technique for the same problem presented a "pressure sensitivity" or instability due to the ineffective imposition of the downstream boundary condition and could not account for separation ahead of the slot. The present study removes these two limitations. Solutions to the triple-deck equations are presented for a wide range of wall injection velocities, and the onset of separation is indeed found to occur ahead of the slot.

Introduction

THE general problem of predicting the influence on the flowfield of injecting a secondary fluid into a well-developed boundary layer is of great practical significance. For example, fluid injection is widely used in the aircraft engine industry for reducing heat transfer across turbine blades and is an effective means of controlling transition or separation (blowoff) of boundary layers over airplane control surfaces. This paper addresses the particular case of strong slot injection into a high Reynolds number supersonic laminar boundary layer over a flat plate, within the framework of the triple-deck theory of Stewartson et al.[1-4] The injection velocity and the slot length are therefore assumed to be respectively of order $Re^{-3/8}\tilde{U}_\infty$ and $Re^{-3/8}\tilde{x}_0$. $\tilde{U}_\infty$ is the freestream velocity, $\tilde{x}_0$ the length of the plate preceding the slot, and Re the asymptotically large Reynolds number, $Re=\tilde{U}_\infty\tilde{x}_0/\tilde{\nu}$, $\tilde{\nu}$ being the kinematic viscosity and the superscript $\sim$ indicating physical quantities. For these conditions three regions or decks are identified around the slot: the lower, middle, and outer decks, characterized by viscous, inviscid rotational, and inviscid irrotational flow conditions and having characteristic heights of order $Re^{-5/8}\tilde{x}_0$, $Re^{-1/2}\tilde{x}_0$, and $Re^{-3/8}\tilde{x}_0$ respectively. For a detailed review of the triple-deck theory and its most important applications, see Ref. 2.

Smith and Stewartson[3,4] consider the problem of slot as well as plate injection into a supersonic laminar boundary layer. They provide a comprehensive review of the literature, formulate a rigorous asymptotic analysis for the strong injection problem, and analyze the connections of their theory with the problem of weak and massive blowing. For the case of strong blowing by slot injection, of interst here, Ref. 3 provides analytical solutions for the linearized equations, valid when the injection velocity is small in the triple-deck scaling, as well as a numerical technique for the full nonlinear problem. However, such a numerical technique presents a "pressure sensitivity," or instability, due to, as the authors themselves acknowledge, the lack of effectively accounting for the downstream boundary condition. Furthermore, it cannot account for boundary layer separation ahead of the slot, most likely to occur for large injection velocities as anticipated by the authors[3] and numerically verified by Werle[5] for a finite value of the Reynolds number. The aim of the present paper is to remove these two difficulties by providing a numerical technique which effectively accounts for the appropriate downstream boundary condition and properly predicts the onset of separation. A detailed study of the slot injection problem for a finite value of the Reynolds number has been recently presented by Werle,[5] who solved the interacting boundary-layer equations in Levy Lees variables with the numerical technique of Werle and Vatsa[6] from which the present one has been derived. In a sense, therefore, this study is the entension of Werle's work[5] to very high Reynolds numbers. In addition, while Werle did not account for the ressure gradient discontinuities across the slot leading and trailing edges produced by a uniform injection velocity, here such a refinement has been successfully introduced on the line suggested in Refs. 5 and 7.

Presented as Paper 79-0142 at the AIAA 17th Aerospace Sciences Meeting, New Orleans, La., Jan. 15-17, 1979; submitted Feb. 21, 1979; revision received July 19, 1979. Copyright © American Institute of Aeronautics and Astronautics, Inc., 1979. All rights reserved. Reprints of this article may be ordered from AIAA Special Publications, 1290 Avenue of the Americas, New York, N.Y. 10019. Order by Article No. at top of page. Member price $2.00 each, nonmember, $3.00 each. **Remittance must accompany order.**

Index categories: Computational Methods; Supersonic and Hypersonic Flow.

*Research Associate, Aerospace Engineering and Applied Mechanics Dept.; currently Assistant Professor, Istituto di Macchine, via Re David 200, 70125, Bari, Italy. Member AIAA.

Governing Equations

The problem of interest is that of laminar supersonic flow of a Newtonian fluid past a flat plate. At a distance $\tilde{x}_0$ from the leading edge of the plate, fluid is injected into the boundary layer with a normal velocity $\tilde{v}_w$ of order $\epsilon^3\tilde{U}_\infty$ through a slot length, $\tilde{x}_s-\tilde{x}_0$, of order $\epsilon^3\tilde{x}_0$, where $\epsilon^8=1/Re$. For this situation, the triple-deck theory of Stewartson and Williams[1] holds almost intact. Independent and dependent variables are nondimensionalized according to the following scalings:

$$\tilde{x}=\tilde{x}_0+\tilde{x}_0\frac{C^{3/8}(\tilde{T}_w/\tilde{T}_\infty)^{3/2}}{\lambda^{5/4}(M_\infty^2-1)^{3/8}}\epsilon^3 x \tag{1}$$

$$\tilde{y}=\tilde{x}_0\frac{C^{5/8}(\tilde{T}_w/\tilde{T}_\infty)^{3/2}}{\lambda^{3/4}(M_\infty^2-1)^{1/8}}\epsilon^5 y \tag{2}$$

$$\tilde{u}=\tilde{U}_\infty\frac{\lambda^{1/4}C^{1/8}(\tilde{T}_w/\tilde{T}_\infty)^{1/2}}{(M_\infty^2-1)^{1/8}}\epsilon u \tag{3}$$

$$\tilde{v}=\tilde{U}_\infty\lambda^{3/4}(M_\infty^2-1)^{1/8}C^{3/8}(\tilde{T}_w/\tilde{T}_\infty)\epsilon^3 v \tag{4}$$

$$\tilde{p}=\tilde{p}_\infty+\tilde{\rho}_\infty\tilde{U}_\infty^2\lambda^{1/2}(M_\infty^2-1)^{-1/4}C^{1/4}\epsilon^2 p \tag{5}$$

In Eqs. (1-5), x,y,u, and v are the longitudinal and normal coordinates and velocity components respectively; p is the pressure, ρ the density, M the Mach number, T the tem-

perature, μ the viscosity coefficient, $C=\tilde{\mu}_w\tilde{T}_\infty/\tilde{\mu}_\infty T_w$ is the Chapman constant, and $\lambda=0.332$ is the Blasius skin friction coefficient. Subscripts ∞ and w indicate freestream and wall conditions, respectively.

Equations (1-5) are then substituted into the compressible Navier Stokes equations and, to first order in the perturbation parameter ϵ, the following triple-deck equations are obtained:

$$u_x+v_y=0 \tag{6a}$$

$$uu_x+vu_y=-\frac{dp}{dx}+u_{yy} \tag{6b}$$

with boundary conditions

$$u(x,0)=0 \tag{7}$$

$$v(x,0)=\begin{cases}0 \text{ for } x\le O \text{ and } x>x_s\\ V_w \text{ elsewhere}\end{cases} \tag{8}$$

$$u(x,y\to\infty)\to y-\delta \tag{9}$$

and the initial condition

$$u(x\to-\infty,y)\to y \tag{10}$$

In the momentum equation (6b) the pressure gradient dp/dx is related to the displacement thickness profile δ by the following linear inviscid interaction law:

$$\frac{dp}{dx}=\frac{d^2\delta}{dx^2} \tag{11}$$

Because of Eq. (11), the triple-deck fundamental problem given by Eqs. (6-11) is of the boundary value type. A boundary condition is therefore required for p (or δ equivalently) at upstream as well as downstream infinity. Here:

$$\delta(x\to-\infty)=0 \tag{12a}$$

$$p(x\to+\infty)=0 \tag{12b}$$

Numerical Method

The numerical technique of Napolitano et al.[8] has been adopted to the present problem of strong slot injection into a supersonic laminar boundary layer. Here, only an outline of the method will be given, together with a detailed description of the differences between the present scheme and the one used in Refs. 8 and 9. A relaxation-like time derivative for the displacement thickness is first added to the right hand side of the momentum equation [Eq. (6b)] to give

$$uu_x+vu_y=-\frac{dp}{dx}+u_{yy}+\frac{\partial\delta}{\partial t} \tag{13}$$

Then a two-sweep alternating direction implicit (ADI) procedure is used to relax the equations in time until convergence is achieved. In the two sweeps, the solution is advanced from time t^n to time $t^*=t^n+\Delta t/2$ and then from t^* to $t^{n+1}=t^*+\Delta t/2$, by writing the respective momentum equations as:

$$(uu_x+vu_y-u_{yy})^*=-\left(\frac{dp}{dx}\right)^n+\lambda(\delta^*-\delta^n) \tag{14a}$$

$$(uu_x+vu_y-u_{yy})^*=-\left(\frac{dp}{dx}\right)^{n+1}+\lambda(\delta^{n+1}-\delta^*) \tag{14b}$$

where $\lambda=2/\Delta t$. In practice the numerical algorithm proceeds as follows. In the first sweep, the pressure gradient $(dp/dx)^n$ is a known function and Eq. (14a) is solved numerically coupled to continuity Eq. (6a) to provide u^*, v^*, and δ^*. In the second sweep, the δ^{n+1} distribution is obtained by solving numerically the following equation

$$\left(\frac{d^2\delta}{dx^2}\right)^{n+1}-\lambda\delta^{n+1}=\left(\frac{dp}{dx}\right)^n-\lambda(2\delta^*-\delta^n) \tag{15}$$

which is obtained by equating the right-hand sides of Eqs. (14a) and (14b) and replacing $(dp/dx)^{n+1}$ with $(d^2\delta/dx^2)^{n+1}$ according to the interaction law, Eq. (11). The $n+1$ time level pressure gradient is finally evaluated as

$$\left(\frac{dp}{dx}\right)^{n+1}=\left(\frac{dp}{dx}\right)^n+\lambda(\delta^{n+1}-2\delta^*+\delta^n) \tag{16}$$

and the whole process is repeated until a satisfactory convergence criterion is met. Note that Eq. (15) is the one which properly accounts for the boundary value nature of the problem by imposing a downstream boundary condition for δ^{n+1} at every second sweep of the iteration process. In the Smith and Stewartson[3] numerical technique this boundary condition was instead satisfied only at the end of the iterative solution process, which therefore developed a "pressure sensitivity," or instability, equivalent to the branching phenomenon of the hypersonic strong interaction problem.[10]

Solution of the * Sweep Equations

The continuity and momentum equations (6a) and (14a) are centered at points C and M, respectively, of the computational domain given in Fig. 1, in order to use the very fast Davis[11] coupled scheme and to obtain second-order accuracy in the normal y direction; the equations are written in finite difference form as follows:

Continuity:

$$\left(\frac{u^*_{i,j}-u^*_{i-1,j}}{x_i-x_{i-1}}+\frac{u^*_{i,j-1}-u^*_{i-1,j-1}}{x_i-x_{i-1}}\right)\frac{1-CW}{2}+\left(\frac{u^0_{i+1,j}-u^*_{i,j}}{x_{i+1}-x_i}+\frac{u^0_{i+1,j-1}-u^*_{i,j-1}}{x_{i+1}-x_i}\right)\frac{CW}{2}+\frac{v^*_{i,j}-v^*_{i,j-1}}{\Delta y}=0 \tag{17}$$

Momentum:

$$u^0_{i,j}\left[\frac{u^*_{i,j}-u^*_{i-1,j}}{x_i-x_{i-1}}(1-CW)+\frac{u^0_{i+1,j}-u^*_{i,j}}{x_{i+1}-x_i}CW\right]+v^*_{i,j}\frac{u^0_{i,j+1}-u^0_{i,j-1}}{2\Delta y}=-\left(\frac{dp}{dx}\right)^n_i+\frac{u^*_{i,j+1}-2u^*_{i,j}+u^*_{i,j-1}}{\Delta y^2}+\lambda\delta^*_i-\lambda\delta^n_i \tag{18}$$

CW is a windward differencing coefficient, equal to 0 if $u^0_{i,j}$ is positive and to 1 if $u^0_{i,j}$ is negative, thus providing automatic windward differencing of the longitudinal convective term in Eq. (18) and of the longitudinal derivative in the continuity

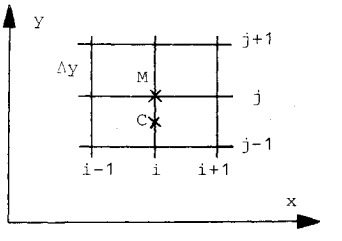

Fig. 1 Computational grid.

Eq. (17). The superscript 0 indicates values taken from the previous * time level. Note that the finite difference Eqs. (17) and (18) allow for a variable grid distribution in the longitudinal x direction, which is a new feature with respect to Refs. 8 and 9. Also, the continuity Eq. (17) is centered here at the x_i location and the nonlinear convective terms of the momentum Eq. (18) are linearized in time, instead of in space. In this way the discontinuities in the u_x and v values at the two edges of the slot are accommodated automatically, and windward differencing of the continuity Eq. (17) is possible. As in Refs. 8 and 9, the longitudinal and normal velocity components at the current time (*) and location (i), $u^*_{i,j}$ and $v^*_{i,j}$, are split as follows:

$$u^*_{i,j} = U_j + \delta^*_i \bar{u}_j \tag{19a}$$

and

$$v^*_{i,j} = V_j + \delta^*_i \bar{v}_j \tag{19b}$$

Equations (19a, b) are then introduced into Eqs. (17) and (18), and the resulting two sets of coupled linear algebraic equations for U_j, V_j, $\bar{u}_j$, and $\bar{v}_j$ for $(j=1,J)$ are efficiently solved by Davis coupled scheme.[11] All the details of the solution procedure are given in Ref. 9. The wall ($j=1$) boundary condition for the normal velocity component, given by Eq. (8) as

$$v^*_{i,j} = V_{w,i} \tag{20}$$

is satisfied by imposing

$$V_1 = V_{w,i} \tag{21a}$$

$$\bar{v}_1 = 0 \tag{21b}$$

In order to properly account for the discontinuous injection velocity profile $V_{w,i}$ ($V_{w,i}=0$ at all the grid points located on the solid wall and $V_{w,i}=V_w$ at those on the slot), a grid point was always made to coincide with either edge of the slot. Also, these two grid points must be assumed to lie on the same side of each edge for consistency. In this study, they were taken to be immediately ahead of it so that $V_{w,I1}=0$ and $V_{w,I2}=V_w$ where the x_{I1} and x_{I2} grid points coincide with the slot leading and trailing edges, respectively.

After the solution for U_j, V_j, $\bar{u}_j$, and $\bar{v}_j$ is obtained at all the y_j locations, the value δ^*_i is found by imposing boundary condition Eq. (9) at the last grid point y_J; $u^*_{i,j}$ and $v^*_{i,j}$ are then recovered by means of Eqs. (19a) and (19b) and the solution process is advanced to the next location x_{i+1}.

Solution to the $n+1$ Sweep Equation

The second sweep equation (15) is written in finite difference form as

$$\frac{2}{(x_{i+1}-x_{i-1})(x_i-x_{i-1})}\delta^{n+1}_{i-1} - \left[\frac{2}{x_{i+1}-x_{i-1}}\left(\frac{1}{x_{i+1}-x_i} + \frac{1}{x_i-x_{i-1}}\right)+\lambda\right]\delta^{n+1}_i + \frac{2}{(x_{i+1}-x_{i-1})(x_{i+1}-x_i)}\delta^{n+1}_{i+1}$$
$$= \left(\frac{dp}{dx}\right)^n_i - \lambda(2\delta^*_i - \delta^n_i) \tag{22}$$

where the variable grid finite difference representation for $(d^2\delta/dx^2)^{n+1}$ has been taken from Blottner.[11]

Equation (22) is straightforwardly solved by the Thomas algorithm with boundary condition Eqs. (12a) and (12b) imposed at the first and last x_i locations, respectively, as:

$$\delta_1 = 0 \tag{23a}$$

$$\left(\frac{d\delta}{dx}\right)_I = \delta_I - \delta_{I-1} = 0 \tag{23b}$$

Note that boundary condition (12b) has been used here in place of its equivalent $\delta(x\to\infty)\to 0$ because $p(x)=d\delta/dx$ decays to zero as $x\to\infty$ faster than δ. Such a higher decay rate obviously leads to higher accuracy when the asymptotic boundary conditions are imposed at a finite distance x_I, as in the present study. Actually, imposing $\delta_I=0$ was found here to produce highly inaccurate results, probably because of the resulting constriction on the injected flow, which was not allowed to be washed away downstream. Boundary condition Eq. (23b) was instead found to be fully satisfactory for all present calculations.

Numerical Accommodation of Pressure Gradient Discontinuities

A special treatment of the second sweep Eq. (15) is required at the two grid points coinciding with the leading and trailing edges of the slot. At either such location the pressure gradient dp/dx and the displacement curvature $d^2\delta/dx^2$ [see Eq. (11)] are discontinuous, that is:

$$\left(\frac{dp}{dx}\right)_{0+} = \left(\frac{dp}{dx}\right)_{0-} + K_0 \tag{24a}$$

and

$$\left(\frac{d^2\delta}{dx^2}\right)_{0+} = \left(\frac{d^2\delta}{dx^2}\right)_{0-} + K_0 \tag{24b}$$

In Eqs. (24a, b), the subscript 0 indicates either point of discontinuity (for convenience) and the superscripts − and + refer to locations immediately to the left and right of it.

Since the grid points in the computational domain have been chosen to coincide with the 0− location, the three point finite difference representation of δ_{xx} used in Eq. (22) must be modified in order to correctly approximate $(\delta_{xx})_{0-}$. For this purpose a Taylor series expansion is written around the 0 location to the right and to the left as follows:

$$\delta_I = \delta_0 + \left(\frac{d\delta}{dx}\right)_0 (x_I - x_0) + \left(\frac{d^2\delta}{dx^2}\right)_{0+} \frac{(x_i-x_0)^2}{2} + \ldots \tag{25a}$$

and

$$\delta_{-1} = \delta_0 + \left(\frac{d\delta}{dx}\right)_0 (x_{-1} - x_0) + \left(\frac{d^2\delta}{dx^2}\right)_{0-} \frac{(x_{-1}-x_0)^2}{2} + \ldots \tag{25b}$$

By combining Eqs. (25a), (25b), and (24b) to eliminate $(d\delta/dx)_0$ and $(d^2\delta/dx^2)_{0+}$, the following appropriate finite difference representation for $(d^2\delta/dx^2)_{0-}$ is obtained.

$$\left(\frac{d^2\delta}{dx^2}\right)_{0-} = \frac{2}{x_1-x_{-1}}\left(\frac{\delta_1-\delta_0}{x_1-x_0} - \frac{\delta_0-\delta_{-1}}{x_0-x_{-1}}\right) - K_0\frac{x_1-x_0}{x_1-x_{-1}} \tag{26}$$

Note that δ and $d\delta/dx$ are continuous through 0 and that Eq. (26) is first-order accurate in Δx if $(d^2\delta/dx^3)_{0+} - (d^3\delta/dx^3)_{0-}$ is finite. The present approach has been already successfully used in Ref. 7 for the solution of the viscous shock layer equations past a spherically blunted cone for which the surface curvature is discontinuous across the sphere-cone juncture. Here, the additional difficulty that the pressure gradient jump K_0 is not known a priori must be accommodated. K_0 is therefore obtained numerically by extrapolation of the n time level pressure gradient profile as follows:

$$K_0 = \left(\frac{dp}{dx}\right)^n_1 + \left[\left(\frac{dp}{dx}\right)^n_1 - \left(\frac{dp}{dx}\right)^n_2\right]\frac{x_1-x_0}{x_2-x_1} - \left(\frac{dp}{dx}\right)^n_{0-} \tag{27}$$

Equation (26), with K_0 given by Eq. (27), is used in the second sweep Eq. (22) at either slot edge grid point, thus allowing for a proper representation of the discontinuous dp/dx profile. The correctness of this approach will be verified in the results section.

Stretching of the Longitudinal Coordinate

The present numerical technique has been seen to use a variable grid in the longitudinal direction x. In the present problem, the solution varies very rapidly in and around the slot region, whereas it has a very slow variation upstream and downstream of the slot. Therefore the following stretching of the longitudinal x coordinate was employed:

$$\bar{x}=x \qquad \text{for } 0\le x\le x_s \qquad (28a)$$

$$\bar{x}-\frac{x_s}{2}=K_1\left(x-\frac{x_s}{2}\right)^2+K_2 \qquad \text{for } x>x_s \qquad (28b)$$

and

$$\bar{x}-\frac{x_s}{2}=-K_1\left(x-\frac{x_s}{2}\right)^2-K_2 \qquad \text{for } x<0 \qquad (28c)$$

The constants K_1 and K_2 are obtained by requiring that at $x=x_s$ (the end of the slot) Eq. (28b) produces $\bar{x}=x_s$, and its derivative $(d\bar{x}/dx)_{x_s}=K_1x_s$ equals 1. Note that for these values of K_1 and K_2 Eq. (28c) and its derivative also give $\bar{x}=x$ and $(d\bar{x}/d\bar{x})_0=1$ at the beginning of the slot, $x=0$.

Transformations (28a) and (28b) produce, for a constant step size in the original x coordinate, a step size in the stretched coordinate $\bar{x}$, which is constant ($\Delta\bar{x}=\Delta x$) inside the slot ($0\le x\le x_s$) and gradually grows ($\Delta\bar{x}>\Delta x$) outside of it ($x>x_s$ and $x<0$). In the present study, for example, where a slot length $x_s=5$ was considered, so that $K_1=0.2$ and $K_2=1.25$, for an unstretched computational domain in the x direction given by $-8\le x\le 13$, the stretching allows one to move the limit of numerical integration as far as -20.8 and $+25.8$ with the same number of grid points. Thus, for the same level of accuracy (same values of x_1 and x_l) the variable grid reduced the computational effort by more than 50%. The bar over the stretched coordinate will be dropped from now onward for convenience.

Results

In the present study, results for only one slot length ($x_s=5$) will be presented. Such a length was chosen because it is one of the two cases for which Smith and Stewartson[3] provide a nonlinear solution and is the one for which Werle[5] presents his finite Re calculations. In this way, the capability of the present scheme of resolving the difficulties of the Smith and Stewartson[3] numerical technique can be tested, and an assessment of the Reynolds number influence is provided. The scheme has been verified to be able to treat different slot lengths as well.

First, a small wall injection velocity, $V_w=0.1$, was considered in order to compare the present results with those given by the linearized equations.[3] Such a comparison was particularly important in order to verify the validity of the pressure gradient discontinuities treatment previously described. In Fig. 2 the pressure obtained with the present scheme for $V_w=0.1$ is compared with the linear solution ($V_w\ll 1$) obtained by numerically evaluating the integrals of Ref. 3. The agreement is excellent, and the pressure gradient discontinuity appears to have been captured very satisfactorily. A step-size study was performed in order to fully assess the reliability and accuracy of the present technique. Figure 3 shows a normal and longitudinal step-size study for the pressure at the beginning of the slot ($x=0$). The pressure indicated by I is obtained by standard Euler integration of the pressure gradient dp/dx. Those indicated by II and III are obtained by a forward and backward first-order difference representation of $d\delta/dx$, respectively. If δ and $d\delta/dx=p$ are continuous across the slot leading edge (whereas $d^2\delta/dx^2=dp/dx$ is discontinuous), $(\delta_1-\delta_0)/(x_1-x_0)$ and $(\delta_0-\delta_{-1})/(x_0-x_{-1})$ should both linearly approach the exact $p(0)$ value, as $\Delta x\to 0$. Figure 3 shows that this is indeed the case. The three pressures all tend to the same limit linearly as $\Delta x\to 0$. Also, such a limit value is seen to be within less than 1% from the linear result (also indicated in Fig. 3). It appears though that a very small step size Δx is necessary in order to obtain accurate solutions; for $\Delta x=0.25$, the three values of pressure differ from the extrapolated "exact" result by as much as 15%. In the present study, all the values plotted in Figs. 2 and 4-6 have been obtained by linearly extrapolating to

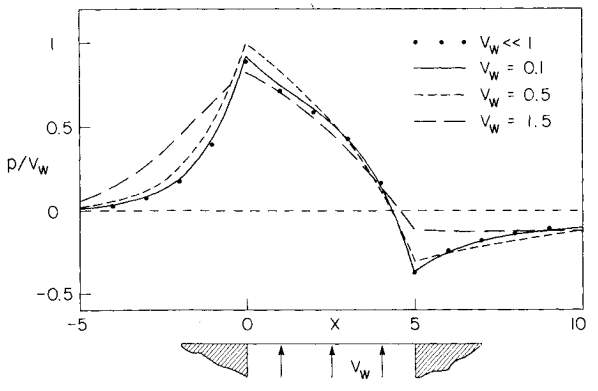

Fig. 2 Normalized pressure profiles.

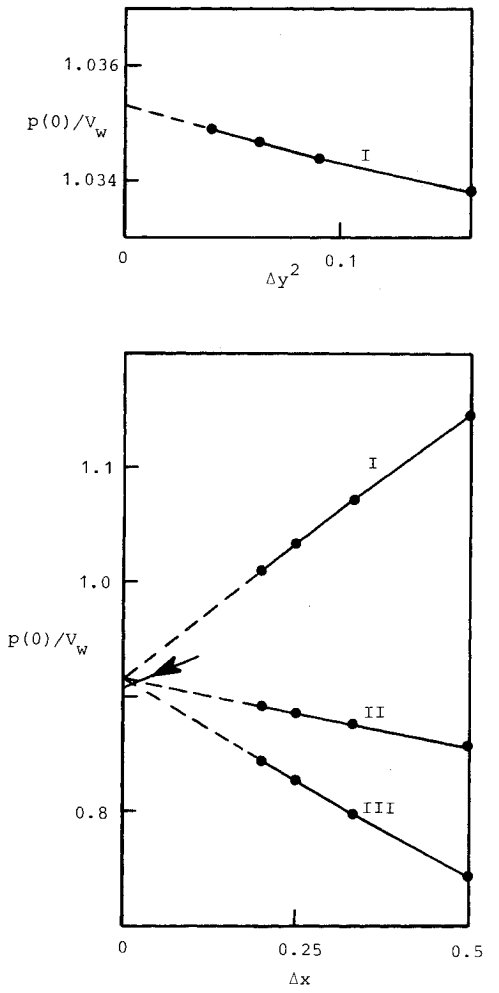

Fig. 3 Step size studies.

$\Delta x = 0$ the numerical solutions obtained for $\Delta x = 0.25$ and $\Delta x = 0.2$.

Figure 3 also shows that the scheme is second-order accurate in the normal direction y and that a step size $\Delta y = 0.3$ provides very accurate results (within 0.1% from the extrapolated to $\Delta y = 0$ value). A constant Δy step size ($\Delta y = 0.3$) was thus used throughout. All the results presented are believed to be accurate within plotting accuracy.

The most important reason for presenting a numerical technique for the full set of nonlinear equations is to be able to predict the onset of separation. Solutions were therefore obtained for various values of V_w. Figure 4 shows the wall shear profile (obtained by a second-order accurate, three-point finite difference representation for $\partial u/\partial y$) corresponding to $V_w = 0.1$, 0.5, and 1.5. The $V_w = 0.1$ profile essentially reproduces all the features of the Smith and Stewartson[3] linear solution. The $V_w = 0.5$ profile is very interesting in that it allows an important point to be made. The only nonlinear solution provided in Ref. 3 is for a value $V_w = 0.4677$. This solution is very similar and close to the one (for $V_w = 0.5$) presented in Fig. 4 and, in particular, shows the same behavior immediately after the leading and trailing edges of the slot. Such behavior is due to the origin of a Goldstein sublayer at each of these two points, and in Ref. 3 a special scaling of the y variable near $y = 0$ was found necessary to resolve these fine flow details. Figure 4 clearly shows that the present scheme, by maintaining second-order accuracy in the y direction and properly accounting for the slot edge discontinuities, is perfectly capable of capturing this fine structure of the solution, even with a constant Δy. Finally, the $V_w = 1$ and 1.5 profiles show the effect of increasing the wall injection velocity on the wall shear. In particular, for the highest value ($V_w = 1.5$) separation occurs ahead of the slot as anticipated in Ref. 3 (where such a feature could not be handled) and found by Werle[5] at a finite value of Re.

Figures 2 and 5 show the pressure and displacement profiles (for $V_w = 0.1$, 0.5, and 1.5) normalized with respect to V_w. As for the case of flow past a parabolic hump,[8,9] linear theory results are seen to hold over a wide range of V_w. The nonlinear results provide only slightly higher values of p and δ for $V_w = 0.5$. For $V_w = 1.5$, separation is seen to smooth the displacement body, thus producing a somewhat flatter pressure distribution.

All the present results qualitatively agree with Werle's[5] finite Re results. A more detailed study of the effect of V_w on the peak pressure value $p(0)$ was pursued in order to make a more precise assessment on the Reynolds number effects.

Figure 6 provides a comparison between the present results [$p(0)$ vs V_w] and those obtained by Werle.[5] The linear and nonlinear results of Smith and Stewartson[3] are also reported for completeness.

The present results show that linear theory underestimates $p(0)$ or $V_w < 1.1$ overestimates $p(0)$ for $V_w > 1.1$. Whereas the present results agree very well with those available from Smith and Stewartson,[3] those given by Werle[5] are markedly higher, especially in the range of $V_w > 0.5$. Incidentally, the present results predict incipient separation for $V_w = 1.1$, whereas Werle[5] found separation at $V_w \simeq 0.8$. It is worth noticing that Werle's results are not extrapolated to zero step size and do not accommodate the pressure gradient discontinuities at the slot edges; they are therefore believed to be less accurate than the present ones. However, the major part of the discrepancy is most likely due to the Reynolds number influence. In fact, triple-deck theory has already been found to be reliable only for very high Re values in the case of supersonic flow past a compression corner.[12] For that case, though, the ($Re \to \infty$) triple-deck pressure is higher at the corner but lower downstream of it than any (finite Re) "interacting boundary-layer" value. It would be interesting to obtain interacting boundary-layer results for a wide range of Re to further clarify this point. Werle suggested that the present $p(0)$ vs V_w profile given in Fig. 6 seems to hint at the existence of a pressure plateau, typical of supersonic interaction,[1,2,12] for the slot injection problem as well. It is the intention of the author to improve the present numerical technique in order to be able to compute the results corresponding to higher values of V_w and thus to verify this point of fundamental importance. Presently, in fact, for $V_w > 1.5$, severe convergence difficulties are encountered. Already for $V_w = 1.5$ the time step Δt had to be reduced from 2 (the optimal value for $V_m \leq 1$) to 0.4, in order to obtain convergence. Correspondingly, the number of iterations grew from about 30 for

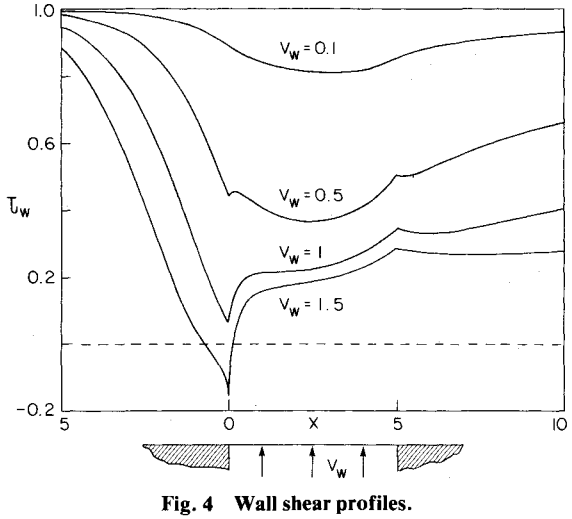

Fig. 4 Wall shear profiles.

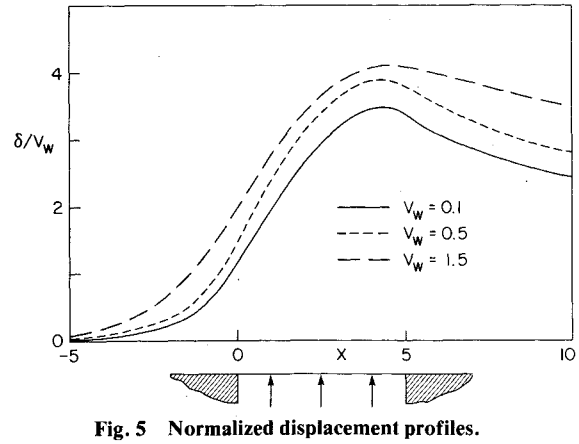

Fig. 5 Normalized displacement profiles.

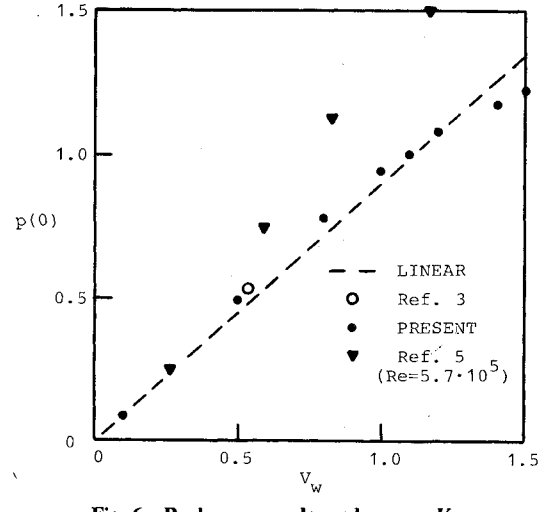

Fig. 6 Peak pressure dependence on V_w.

$V_w = 0.1$, to 100 for $V_w = 1$, and 500 for $V_w = 1.5$. The numerical range of integration was $-20.8 \le x \le 25.8$ throughout, and $0 \le y \le y_J$ with y_J ranging from 12 to 21 with growing V_w.

In all the cases, the u velocity profile was verified to take on a linear growth over several grid points around y_J, and the solution was verified not to change by further increasing the range of integration for x. Each two sets of results ($\Delta x = 0.25$ and $\Delta x = 0.2$) required from about 20 s ($V_w = 0.1$) to 8 min ($V_w = 1.5$) on an AMDAHL 470. For $V_w > 0.1$, V_w was increased by 0.1 at each iteration until the final value was obtained. All the computations were started with a uniform shear flow taken as initial condition. Introduction of a variable grid in the normal direction as well is expected to again halve the computational effort without any loss of accuracy.

Acknowledgment

This research was supported by the Office of Naval Research under Contract ONR-N00014-76-C-0364 and by the Naval Sea Systems Command General Hydromechanics Research Program administered by the David W. Taylor Naval Ship Research and Development Center under Contract N00014-76-C-0359. The author would like to express his sincere appreciation to R. T. Davis and M. J. Werle for their valuable suggestions and comments.

References

[1] Stewartson, K. and Williams, P. G., "Self-Induced Separation," *Proceedings of the Royal Society of London*, Series A, Vol. 312, 1969, pp. 181-206.

[2] Stewartson, K., "Multistructured Boundary Layers on Flat Plates and Related Bodies," *Advances in Applied Mechanics*, Vol. 14, Academic Press, New York, 1974.

[3] Smith, F. T. and Stewartson, K., "On Slot Injection Into a Supersonic Laminar Boundary Layer," *Proceedings of the Royal Society of London*, Series A, Vol. 332, 1973, pp. 1-22.

[4] Smith, F. T. and Stewartson, K., "Plate Injection into a Separated Supersonic Boundary Layer," *Journal of Fluid Mechanics*, Vol. 58, Pt. 1, 1973, pp. 143-159.

[5] Werle, M. J., "Supersonic Laminar Boundary-Layer Separation by Slot Injection," *AIAA Journal*, Vol. 17, Feb. 1979, pp. 160-167.

[6] Werle, M. J. and Vatsa, V. N., "A New Method for Boundary Layer Separation," *AIAA Journal*, Vol. 12, Nov. 1974, pp. 1991-1997.

[7] Srivastava, B. N., Werle, M. J., and Davis, R. T., "Viscous Shock Layer Solutions for Hypersonic Sphere-Cones," *AIAA Journal*, Vol. 16, Feb. 1978, pp. 137-144.

[8] Napolitano, M., Werle, M. J., and Davis, R. T., "A Numerical Technique for the Triple Deck Problem," *AIAA Journal*, Vol. 17, July 1979, pp. 699-705.

[9] Napolitano, M., Werle, M. J., and Davis, R. T., "Numerical Solutions of the Triple-Deck Equations for Supersonic and Subsonic Flow Past a Hump," University of Cincinnati, Dept. of Aerospace Engineering AFL Rept. No. 78-6-42, June 1978.

[10] Werle, M. J. and Wornom, S. F., "Numerical Studies of the Hypersonic Strong Interaction Boundary Layer Equations," *AIAA Journal*, Vol. 9, 1971, pp. 2058-2060.

[11] Blottner, F. G., "Computational Techniques for Boundary Layers," AGARD Lecture Series No. 73, Feb. 1975, pp. 3-9.

[12] Burggraf, O., Rizzetta, D. P., Werle, M. J. and Vatsa, V. N., "Effects of Reynolds Number on Laminar Separation of a Supersonic Stream," *AIAA Journal*, Vol. 17, April 1979, pp. 336-343.

From the AIAA Progress in Astronautics and Aeronautics Series . . .

TURBULENT COMBUSTION—v. 58

Edited by Lawrence A. Kennedy, State University of New York at Buffalo

Practical combustion systems are almost all based on turbulent combustion, as distinct from the more elementary processes (more academically appealing) of laminar or even stationary combustion. A practical combustor, whether employed in a power generating plant, in an automobile engine, in an aircraft jet engine, or whatever, requires a large and fast mass flow or throughput in order to meet useful specifications. The impetus for the study of turbulent combustion is therefore strong.

In spite of this, our understanding of turbulent combustion processes, that is, more specifically the interplay of fast oxidative chemical reactions, strong transport fluxes of heat and mass, and intense fluid-mechanical turbulence, is still incomplete. In the last few years, two strong forces have emerged that now compel research scientists to attack the subject of turbulent combustion anew. One is the development of novel instrumental techniques that permit rather precise nonintrusive measurement of reactant concentrations, turbulent velocity fluctuations, temperatures, etc., generally by optical means using laser beams. The other is the compelling demand to solve hitherto bypassed problems such as identifying the mechanisms responsible for the production of the minor compounds labeled pollutants and discovering ways to reduce such emissions.

This new climate of research in turbulent combustion and the availability of new results led to the Symposium from which this book is derived. Anyone interested in the modern science of combustion will find this book a rewarding source of information.

485 pp., 6 × 9, illus. $20.00 Mem. $35.00 List

TO ORDER WRITE: Publications Dept., AIAA, 1290 Avenue of the Americas, New York, N. Y. 10019